

# Dalton Transactions

Accepted Manuscript



This is an *Accepted Manuscript*, which has been through the Royal Society of Chemistry peer review process and has been accepted for publication.

*Accepted Manuscripts* are published online shortly after acceptance, before technical editing, formatting and proof reading. Using this free service, authors can make their results available to the community, in citable form, before we publish the edited article. We will replace this *Accepted Manuscript* with the edited and formatted *Advance Article* as soon as it is available.

You can find more information about *Accepted Manuscripts* in the [Information for Authors](#).

Please note that technical editing may introduce minor changes to the text and/or graphics, which may alter content. The journal's standard [Terms & Conditions](#) and the [Ethical guidelines](#) still apply. In no event shall the Royal Society of Chemistry be held responsible for any errors or omissions in this *Accepted Manuscript* or any consequences arising from the use of any information it contains.

## ARTICLE

# Cu(II)-Dy(III) and Co(III)-Dy(III) based single molecule magnets with multiple slow magnetic relaxation processes in Cu(II)-Dy(III) complex

Cite this: DOI: 10.1039/x0xx00000x

Received 00th January 2012,  
Accepted 00th January 2012

DOI: 10.1039/x0xx00000x

[www.rsc.org/](http://www.rsc.org/)Malay Dolai<sup>a</sup>, Mahammad Ali<sup>a,\*</sup>, Ján Titiš<sup>b</sup> and Roman Boča<sup>b,\*</sup>

Two dinuclear Schiff-base complexes [Cu<sup>II</sup>Dy<sup>III</sup>] and [Co<sup>III</sup>Dy<sup>III</sup>] have been synthesized and structurally characterized. The AC susceptibility measurements taken at  $B_{DC} = 0.2$  T show a slow magnetic relaxation typical for single-molecule magnets. Unusual is the presence of three relaxation branches in [Cu<sup>II</sup>Dy<sup>III</sup>]; the slowest (low-frequency) process possesses the barrier to spin reversal of  $U/k_B = 2.8$  K and extrapolated relaxation time as slow as  $\tau_0 = 0.11$  s. The intermediate-frequency process is typical for SMM of this class with  $U/k_B = 122$  K and  $\tau_0 = 9.9 \times 10^{-7}$  s; an onset of the high-frequency process is evidenced and this is the fastest. On the contrary, [Co<sup>III</sup>Dy<sup>III</sup>] complex free of exchange coupling, exhibits only a single relaxation path with SMM parameters  $U/k_B = 113$  K,  $\tau_0 = 7.0 \times 10^{-9}$  s.

## Introduction

In recent years, complexes containing 3d–4f metal ions have attracted the attention of chemists and physicists owing to their interesting single-molecule magnet (SMM) behavior, a species characterized by their high spin ground state and negative axial anisotropy.<sup>1</sup> Since the discovery of ferromagnetic interaction between copper(II) and isotropic gadolinium(III) ion within a discrete trinuclear complex<sup>2</sup> the interests towards this field have expanded enormously in recent years. The magnetic anisotropy of an exchange-coupled system depends not only on the individual anisotropies of the metal ions but also on the relative orientation of the local axes.<sup>3</sup> Because of many 4f ions with strong magnetic anisotropy, especially for Tb<sup>III</sup> (<sup>7</sup>F<sub>6</sub>), Dy<sup>III</sup> (<sup>6</sup>H<sub>15/2</sub>), and Ho<sup>III</sup> (<sup>5</sup>H<sub>8</sub>), significant effort is devoted to construct SMMs containing 3d–4f or pure 4f systems.<sup>4,5</sup> In this respect, the design of new lanthanide complexes with new topology might provide a unique opportunity to probe the relaxation dynamics of lanthanide aggregates, thus nickel(II),<sup>7</sup> manganese(II),<sup>8</sup> and iron(III)<sup>9</sup> ions which can bring

enriching the structure correlation to the magnetic properties of the Ln family.

Unfortunately, the study of magnetic interactions between the 3d and 4f metal ions in a complex is not straightforward as several interaction pathways between 3d–3d, 3d–4f, and 4f–4f ions may be operative. On the contrary, the preparation of complexes containing only a fewer number of 3d and 4f ions is crucial when the study is oriented toward a better understanding of the 3d–4f magnetic interactions. In such a case, the best example is a simple heterodinuclear 3d–4f complex, well isolated from its congeners.

Interestingly, only a handful of such complexes with interesting magnetic properties have been reported so far, because of the inherent difficulties encountered during their preparation, mainly due to product scrambling. Most of these reported complexes are based on copper(II),<sup>6</sup>

## ARTICLE

in, along with the lanthanide ions, a larger ground state spin. Surprisingly, however, there is scarcely any report on 3d-4f dimeric compounds involving copper(II) ion<sup>10</sup>, in particular there is no any report on Cu<sup>II</sup>-Dy<sup>III</sup> dinuclear complex; some Cu<sub>3</sub>Dy complexes were reported.<sup>10o,p</sup>

Slow magnetic relaxation is an important property of SMMs that can bring technological applications for information storage and so many others.<sup>1,2</sup> The detailed characterization of such processes is of utmost importance, as it may help to manipulated the magnetic relaxation times through simple alterations of the ligand field. The slow magnetic relaxation may arise in discrete mononuclear molecular magnets that are not typically apparent for multinuclear clusters. In particular, the strong spin-orbit coupling and generally lower spin can facilitate phonon-based relaxation mechanisms involving only the ground state (direct relaxation) or the ground state and some real or virtual excited state (Orbach and Raman relaxation, respectively).<sup>11</sup> To date, however, a limited number of compounds has been shown to exhibit more than one well-resolved pathway for slow magnetic relaxation.<sup>12</sup> In the present article we are going to disclose a simple [Cu<sup>II</sup>Dy<sup>III</sup>] dinuclear complex which exhibits SMM behavior with three slow magnetic relaxation processes. For comparison, also the [Co<sup>III</sup>Dy<sup>III</sup>] dinuclear complex has been prepared and subjected to magnetochemical studies.

## Results and discussion

### Synthesis and Structural description of the complexes **1** and **2**

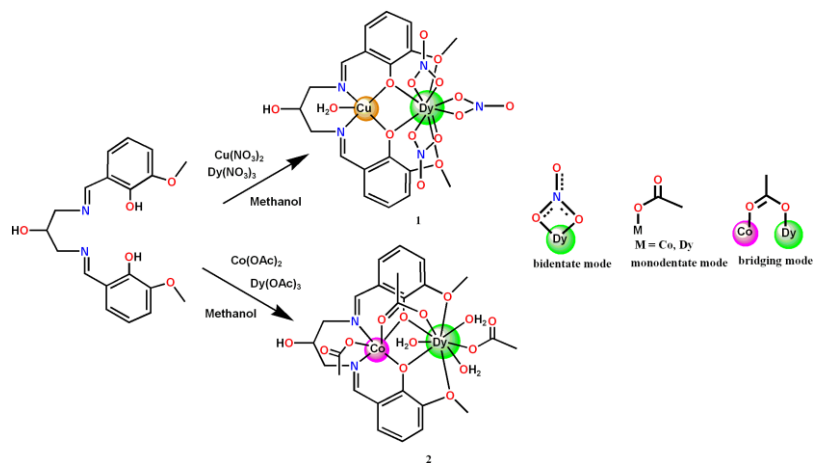
The bi-compartmental ligand, H<sub>3</sub>L was prepared by Schiff base condensation of 2-hydroxy-1,3-diaminopropane

and stronger anisotropy in the resulting compounds. and *o*-vanillin. The dinuclear [Cu<sup>II</sup>Dy<sup>III</sup>] complex was prepared by the reaction of Cu(NO<sub>3</sub>)<sub>2</sub>·6H<sub>2</sub>O with H<sub>3</sub>L in MeOH followed by addition of Dy(NO<sub>3</sub>)<sub>3</sub> and TEA in 1:1:1:2 mole ratio. The corresponding [Co<sup>III</sup>Dy<sup>III</sup>] complex was prepared in a similar manner but here Co(OAc)<sub>2</sub> and Dy(OAc)<sub>3</sub> were used instead of the corresponding nitrate salts as in case of **1**. Use of Co(NO<sub>3</sub>)<sub>2</sub> and Dy(NO<sub>3</sub>)<sub>3</sub> did not yield single crystals of the [Co<sup>III</sup>Dy<sup>III</sup>] complex.

The single crystal X-ray diffraction study reveals that the complex **1** crystallizes in the monoclinic *P21/c* space group. The molecular structure of **1** is depicted in Fig.1 which clearly demonstrates that it is a dinuclear [Cu<sup>II</sup>Dy<sup>III</sup>] species where each metal atom is doubly bridged by two phenolato oxygen atoms of the ligand. The selected bond lengths and bond angles around both metal centers in **1** are given in ESI (Table S1).

The Cu<sup>II</sup> ion in the dinuclear complex reside in the salen-type N<sub>2</sub>O<sub>2</sub> compartment, while the Dy<sup>III</sup> ion is situated at the open and comparatively larger O<sub>4</sub>[O(phenoxido)<sub>2</sub>-O(methoxido)<sub>2</sub>] compartment of the dinucleating bicompartamental ligand HL<sup>2-</sup>. The Cu<sup>II</sup> centre is pentacoordinated, in which the basal plane is formed by N<sub>2</sub>O<sub>2</sub> donor set of atoms of the Schiff-base ligand and the sole apical position is occupied one water molecule (O5), resulting in a square-pyramidal geometry. The apical Cu–O bond length 2.329(7) Å is significantly longer than those found in basal plane (Table 1), which is a signature of the Jahn-Teller distortion, generally found in Cu<sup>II</sup> systems.

## ARTICLE



**Scheme 1:** The schematic representation of the formation of complexes. Coordination modes of nitrate, acetate groups.

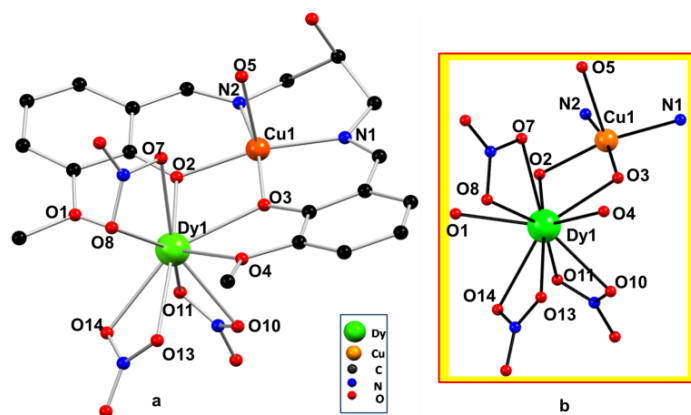


**Fig. 1.**(a) The molecular structure of **1**; (b) Donor set of the metal centers. Hydrogen atoms are omitted for clarity.

On the other hand, Dy<sup>III</sup> ion in **1** is decacoordinated, comprising of four oxygen atoms of O4 compartment and six oxygen atoms from three bidentate nitrate ligands. Interestingly, the bond distances around Dy<sup>III</sup> ion involving phenoxido and methoxido oxygen atoms are comparable; Dy–O(phenoxido) = 2.343(5) – 2.345(4) Å and Dy–O(methoxido) = 2.494(5) – 2.502(5) Å. Similarity in bond lengths involving the coordinated nitrates are also apparent; Dy–O(NO<sub>3</sub><sup>−</sup>) distances fall of in the range 2.452(5) – 2.599 (7) Å. The coordination polyhedron of Dy<sup>III</sup> can be best described by a distorted bicapped square antiprism; the two square planes are defined by O(phenoxido) O(methoxido) O(nitrato)

O(nitrato) and O(methoxido) O(nitrato) O(nitrato) O(nitrato), while O(phenoxido) and O(nitrato) can be considered as the capping atoms (Fig. S1). However, the displacement of Dy<sup>III</sup> from the corresponding least-squares O(phenoxido)<sub>2</sub>O(methoxido)<sub>2</sub> planes are 0.589 Å, suggesting that the Dy<sup>III</sup> ion lies significantly away from the concerning mean plane (Fig. S1). In addition, the non-coordinated –OH groups play a crucial role for the formation of H-bonded supramolecular network (Fig. S2 and Fig. S3).

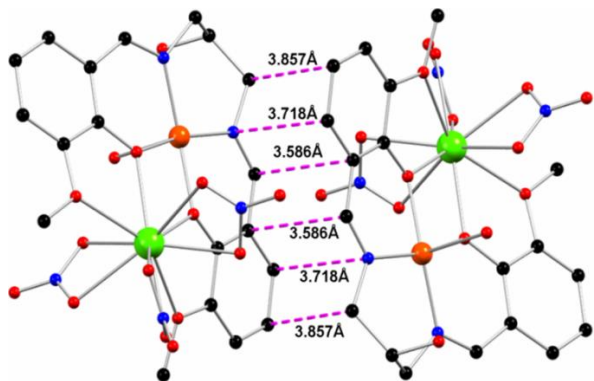


Fig. 2. Short intermolecular contacts for **1** giving rise to weakly coupled  $[\text{Cu}^{\text{II}}\text{Dy}^{\text{III}}]_2$  units.

The complex  $[\text{CoDy}(\text{HL})(\text{AcO})_3(\text{H}_2\text{O})_3] \cdot (\text{AcO})(\text{H}_2\text{O})_3$  (**2**), is also a dinuclear species crystallizing in the monoclinic  $P21/c$  space group. The molecular view of **2** is depicted in Fig. 3. In this dinuclear molecular complex, both the metal centers are doubly bridged by two phenoxido oxygen atoms of the ligand. The selected bond lengths and bond angles around both metal centers in complex **2** are given in Table S4. As usual the  $\text{Co}^{\text{III}}$  ion resides in the inner core while the  $\text{Dy}^{\text{III}}$  ion is in the outer core of the compartmental ligand  $\text{HL}^{2-}$ . The  $\text{Co}^{\text{III}}$  centre is hexacoordinated, the basal plane being constructed by  $\text{N}_2\text{O}_2$  donor set of atoms and the two apical positions are occupied by two acetato ligands (one in  $\eta^1$  fashion and another in  $\eta^2$  fashion being further coordinated to  $\text{Dy}^{\text{III}}$  ion), resulting in a distorted octahedral geometry.

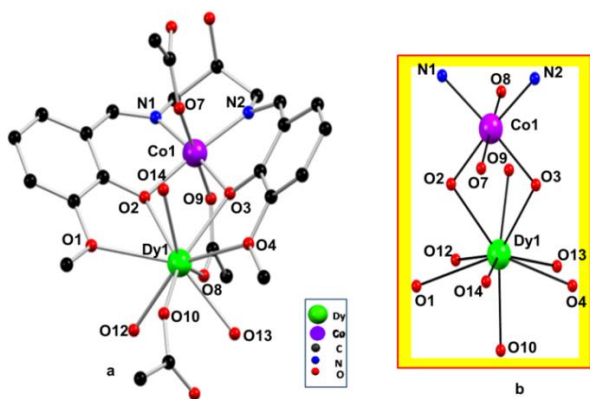


Fig. 3. (a) The molecular structure of **2**; (b) Donor set of the metal centers. Hydrogen atoms, counter anions and crystal water are omitted for clarity.

On the other hand,  $\text{Dy}^{\text{III}}$  ion is nonacoordinated, comprising of four oxygen atoms, two from phenoxido bridging atoms

and other two methoxido oxygen atoms, and other five oxygen atoms come from three aqua ligands (w) and two from two acetato ligands. Interestingly, the bond distances around  $\text{Dy}^{\text{III}}$  ion involving phenoxido and methoxido oxygen atoms are comparable:  $\text{Dy}-\text{O}(\text{phenoxido}) = 2.355(2) - 2.373(2) \text{ \AA}$  and  $\text{Dy}-\text{O}(\text{methoxido}) = 2.596(3) - 2.633(2) \text{ \AA}$  while  $\text{Dy}-\text{O}(\text{w})$  distances fall of in the range  $2.385(3) - 2.430(3) \text{ \AA}$ . The  $\text{Dy}^{\text{III}}-\text{O}(\eta_2-\text{OAc})$  bond distance ( $2.345(2) \text{ \AA}$ ) is longer than  $\text{Dy}^{\text{III}}-\text{O}(\eta_1-\text{OAc})$  bond distance ( $2.262(2) \text{ \AA}$ ). The coordination polyhedron around  $\text{Dy}^{\text{III}}$  can be best described by a distorted monocapped square antiprism; the two square planes are defined by  $\text{O}(\text{phenoxido})\text{O}(\text{methoxido})\text{O}(\eta_2-\text{acetato})\text{O}(\text{w})$  and  $\text{O}(\text{phenoxido})\text{O}(\text{methoxido})\text{O}(\eta_1-\text{acetato})\text{O}(\text{w})$ , while one  $\text{O}(\text{w})$  can be considered as the monocapping atom (Fig. S1). However,  $\text{Dy}^{\text{III}}$  lies significantly away ( $0.934 \text{ \AA}$ ) from the mean plane comprising of  $\text{O}(\text{phenoxido})_2\text{O}(\text{methoxido})_2$  planes (Fig. S1). For balancing the charge on the two metal ions ( $\text{Co}^{\text{III}}$  and  $\text{Dy}^{\text{III}}$ ) one acetate ion is uncoordinated and three water molecules are present outside of the coordination sphere. In addition, the non-coordinated  $-\text{OH}$  groups play a crucial role for the formation of H-bonded supramolecular network (Fig. S4 and Fig. S5).

### Magnetic Data Analysis

The DC magnetization measurements gave the temperature dependence of the magnetic susceptibility (converted to the dimensionless product function  $\chi T/C_0$ ,  $C_0 = N_A \mu_0 \mu_B^2 / k_B$ ) and the field dependence of the magnetization (Fig. 4). The product function is weakly dependent on temperature, except the lowest temperature region where it drops down more rapidly. The room temperature value of  $\chi T/C_0 = 32.7$  is lower than that of the isotropic high-temperature limit calculated as  $\chi T/C_0(\text{HT}) = [g_{\text{Cu}}^2 s_{\text{Cu}}(s_{\text{Cu}} + 1)/3 + g_{\text{Dy}}^2 j_{\text{Dy}}(j_{\text{Dy}} + 1)/3] = 38.9$  ( $j_{\text{Dy}} = 15/2$ ,  $g_{\text{Dy}} = 4/3$  for  $^6\text{H}_{15/2}$  ground multiplet;  $g_{\text{Cu}} = 2.1$ ) probably due to the combined effect of the exchange coupling of an antiferromagnetic nature and single-ion anisotropy of  $\text{Dy}^{\text{III}}$ .<sup>13</sup> The saturation limit of the molar magnetization per formula unit is  $M_1 = M_{\text{mol}}/(N_A \mu_B) = g_{\text{Cu}} s_{\text{Cu}} + g_{\text{Dy}} j_{\text{Dy}} = 11.1$ . Again, one can see that the observed magnetization  $M_1 = 6.1$  is far from this isotropic estimate due to high magnetic anisotropy: the magnetization rises rapidly with the ramping field, and then continues to increase gradually; it is not saturated at  $T = 2.0 \text{ K}$  and  $B = 7 \text{ T}$ .



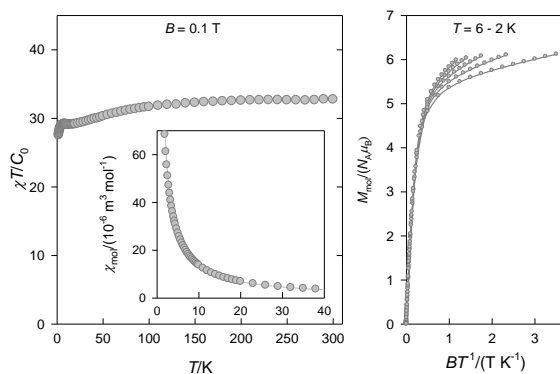


**Fig. 4** Magnetic function for **1** per formula unit  $M_r = 786.46$ . Left - temperature dependence of the product function (dimensionless); inset - molar magnetic susceptibility (SI units); right - magnetization vs  $B/T$ .

The AC susceptibility measurements for the complex **1** are displayed in Fig. S7 for four frequencies of the alternating field at fixed temperature  $T = 2.0$  K where the effect of the external magnetic field to the real (in-phase) and imaginary (out-of-phase) component of the magnetic susceptibility is mapped. At the zero field the out-of-phase component  $\chi''$  is almost zero but with increasing  $B_{DC}$  it rises progressively to a maximum around 0.2 T (depending upon the frequency  $f$  of the AC field). This confirms that the SMM behaviour of the complex depends upon the applied field. The subsequent AC measurements were done at  $B_{DC} = 0.2$  T, respectively.

The temperature evolution of the AC susceptibility components for the complex **1** is displayed in Fig. S8 for thirteen frequencies of the alternating field ranging between  $f = 0.2 - 1512$  Hz and temperature interval  $T = 1.85 - 5.0$  K. It can be seen that the out-of phase component of the molar magnetic susceptibility  $\chi''$  exhibits temperature-dependent course that depends upon the applied frequency. The frequency dependence of out-of phase susceptibility component confirms a superparamagnetic behaviour that is one of the characteristic features of the single molecule magnets.

The magnetic data was replotted as functions of the frequency at the constant temperature as shown in Fig. 5. The out-of phase component evidences the presence of three relaxation processes; the low-frequency (LF) process dominates at the low temperature and the intermediate-frequency (IF) process tends to escape with temperature (above 3.25 K it is oddly visible). The maximum of the high-frequency (HF) process lies far above the hardware limit

(1500 Hz) and it can be estimated only by a fitting procedure (above  $10^5$  Hz).

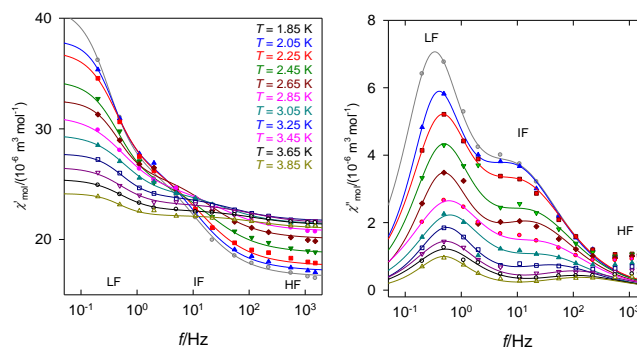


**Fig. 5** (Color online). The AC susceptibility data for **1** at  $B_{DC} = 0.2$  T. Left - frequency dependence of the in-phase molar susceptibility; right - frequency dependence of the out-of-phase molar susceptibility. Solid lines - fitted with a two-component Debye model by omitting three highest frequency data referring to the HF process.

The quantitative processing of the AC data meets a number of difficulties. The key problem lies in the fact that the peaks at  $\chi''$  referring to different relaxation paths are overlapped. In solving this problem, an extended Debye model has been used in interpreting the frequency dependence of the AC magnetic susceptibility in the form

$$\hat{\chi}(\omega) = \chi_S + (\chi_{T1} - \chi_S) / [1 + (i\omega\tau_1)^{-\alpha_1}] + (\chi_{T2} - \chi_{T1}) / [1 + (i\omega\tau_2)^{-\alpha_2}] \quad (1)$$

where, two relaxation times ( $\tau_1, \tau_2$ ) and two distribution parameters ( $\alpha_1, \alpha_2$ ) occur along with two isothermal susceptibilities ( $\chi_{T1}, \chi_{T2}$ ) and the common adiabatic susceptibility ( $\chi_S$ );  $\omega = 2\pi f$ . This equation decomposes into two components as shown in ESI. The fitting procedure has been based upon minimization of a functional  $F = w_1 \cdot \chi'(\omega) + w_2 \cdot \chi''(\omega)$  that accounts to both susceptibility components;  $13 \times 2 = 26$  data points are at the disposal for a fixed temperature. Notice, each peak of  $\chi''$  is fully characterized by three parameters (position -  $f_{max}''$  inversely proportional to the relaxation time, height -  $\chi_T$  and width - related to  $\alpha$ ). Moreover, each wave at  $\chi'$  is again characterized by the same set of parameters (low-frequency limit, slope, and inflection point).

However, this form cannot reproduce three highest frequency points which refer to an on-set of the third relaxation path. To this end, only  $10 \times 2 = 20$  data points were processed using advanced methods of the non-linear optimization (simulated annealing and a genetic algorithm).

The quality of the fit can be monitored as solid lines in Fig. 5, and by statistical characteristics such as the discrepancy factors  $R(\chi)$  and  $R(\chi')$ , and standard deviations of each parameter (Table S7).

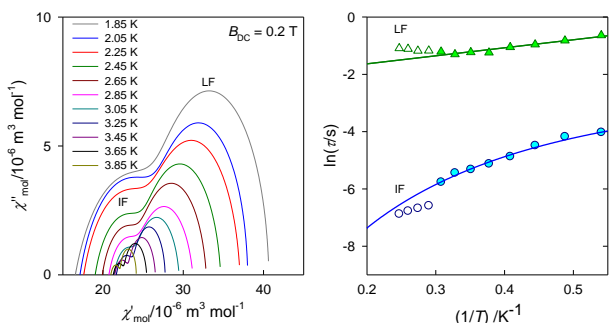


**Fig. 6.** The AC susceptibility data for **1** at  $B_{DC} = 0.2$  T. Left – Argand plot (fixed temperature), lines based upon fitted parameters; right – Arrhenius-like plot with fits based on eqn. (1). Empty symbols – data deleted from the regression.

The out-of-phase susceptibility has been plotted versus the in-phase component and in this way Argand (Cole-Cole) diagram has been constructed in Fig. 6; it consists of two distorted and heavily overlapped semicircles.

The maxima of the primitive curves define two relaxation times  $\tau = 1/(2\pi f''_{max})$  which enter the Arrhenius-like plot ( $\ln \tau$ ) vs  $T^{-1}$  displayed in Fig. 6 – right.

The relaxation time accounting to the Orbach process (parameters  $U$ ,  $\tau_0$ ), direct process (parameters  $A$ ,  $m$ ), and Raman process (parameters  $C$ ,  $n$ ) can be further fitted by using the formula<sup>14</sup>

$$\tau^{-1} = \tau_0^{-1} \exp(-U/k_B T) + AB^m T + CT^n \quad (2)$$

The parameters of the SMM behaviour are listed in Table 1. It can be seen that the IF relaxation process displays characteristics that are typical for other SMM, at least the SMM composed of dysprosium central atom ( $\tau_0 = 10^{-6} - 10^{-11}$  s).<sup>15</sup> However, the LF relaxation process is as slow as  $\tau_0 = 0.11$  s. The characteristics of the HF relaxation process referring to an extrapolation show that this process is the fastest.

The presence of three relaxation processes with different relaxation times is a challenge and probably it is unprecedented. We can only speculate what might be a reason of this. As the formation of dimers  $[\text{CuDy}]_2$  with short contacts is confirmed, we assume that the LF relaxation branch is associated with the relaxation of a dimeric unit  $[\text{CuDy}]_2$  and that of the IF refers the dinuclear monomer

$[\text{CuDy}]$ . The HF relaxation could be ascribed to the individual  $\text{Dy}^{\text{III}}$  centres and it resembles the spin glass behaviour.

**Table 1.** Parameters of the SMM behaviour for **1** and **2**.

Parameter	<b>1</b> , LF	<b>1</b> , IF	<b>2</b>
$U/k_B/K^{-1}$	2.8	122(1)	113(7)
$\tau_0/s$	0.112	$9.9(1) \times 10^{-7}$	$7.0(43) \times 10^{-9}$
$A/T^m/K^{-1} s^{-1}$		$9.3 \times 10^4$	838
$m$		4	4
$C/K^{-n} s^{-1}$		2.40	0.067(28)
$n$		4	4.5(2)

The DFT calculations have been done with improved algorithm. The energy levels calculated by this method are deposited in ESI (Table S9) The strength of the exchange coupling has been estimated by applying the DFT calculations in the experimental geometry of the  $[\text{Cu}^{\text{II}}\text{Dy}^{\text{III}}]$  complex with the spin multiplicity  $m = 7$ : the Yamaguchi formula gave  $J/hc = -2.83 \text{ cm}^{-1}$ .<sup>16</sup>

In order to filter off the effect of the exchange coupling to the magnetic behaviour and slow magnetic relaxation, an attempt to substitute the  $\text{Cu}^{\text{II}}$  centre with a diamagnetic analogue has been done. For this purpose the  $[\text{Co}^{\text{III}}\text{Dy}^{\text{III}}]$  complex, **2**, has been prepared and structurally characterized. However, a perfect structural analogue is difficult to achieve, since the  $\text{Cu}^{\text{II}}$  central atom prefers pentacoordination while in the  $\text{Co}^{\text{III}}$  analogue a hexacoordination appears. The same obstacle will be met by the  $\text{Zn}(\text{II})$  substitution since hard Lewis acid would prefer hexacoordination.

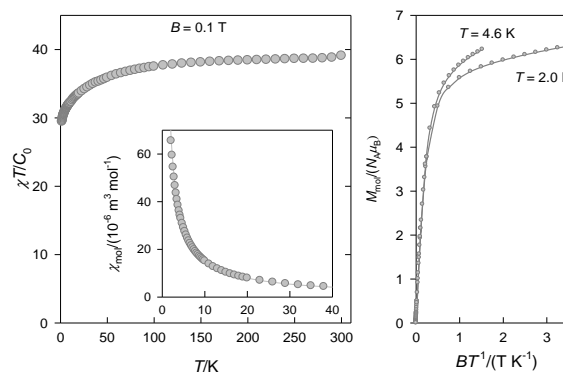


**Fig. 7.** Magnetic function for **2** per formula unit  $M_r = 922.07$ . Left - temperature dependence of the product function (dimensionless); inset – molar magnetic susceptibility (SI units); right – magnetization vs  $B/T$ .

DC magnetic data for **2** is shown in Fig. 7. It is seen that the room-temperature value of the product function adopts a value of  $\chi T/C_0 = 39.0$  that is close to the high-temperature limit  $\chi T/C_0(\text{HT}) = g_{\text{Dy}}^2 j_{\text{Dy}}(j_{\text{Dy}} + 1)/3 = 37.8$  ( $j_{\text{Dy}} = 15/2$ ,  $g_{\text{Dy}} = 4/3$

for  ${}^6\text{H}_{15/2}$  ground multiplet). Now the net effect of the magnetic anisotropy is seen at low-temperature part of the product functions as well as on the magnetization vs  $B/T$  functions.

The AC susceptibility data for **2** has been taken and processed in an analogy with **1** (Fig. S10). Fig. 8 brings the frequency dependence of the susceptibility components confirming that only a single relaxation process exists in **2**. However, the peaks at the lowest temperature are a bit asymmetric so that the fitting procedure using the extended Debye model with  $\alpha$ -parameter is partly successful. The corresponding Arrhenius-like plot is drawn in Fig. 9. The fitting procedure via eqn. (2) yields the parameters listed in Table 1.

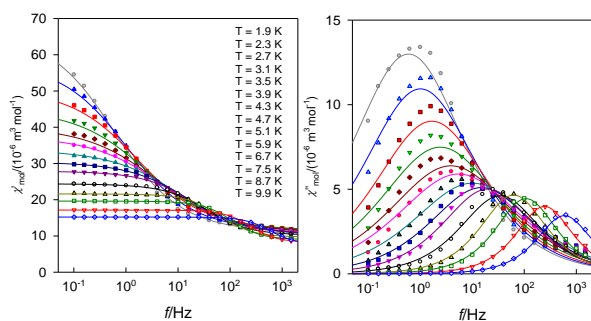


**Fig. 8** The AC susceptibility data for **2** at  $B_{\text{DC}} = 0.2$  T. Solid lines – fitted.

A comparison of the relaxation data for **1** and **2** (at the same external field  $B_{\text{DC}} = 0.2$  T) shows that the very slow relaxation path evident at low temperature for **1** ( $U/k_{\text{B}} = 2.8$  K,  $\tau_0 = 0.11$  s) disappears in **2**. The second relaxation path in **1** ( $U/k_{\text{B}} = 122$  K,  $\tau_0 = 9.9 \times 10^{-7}$  s) finds its counterpart in **2** ( $U/k_{\text{B}} = 113$  K,  $\tau_0 = 7.0 \times 10^{-9}$  s) whereas the high-frequency (the fastest) relaxation path again disappears. These findings support a hypothesis that the exchange coupling in **1** assists in the slowest relaxation process.

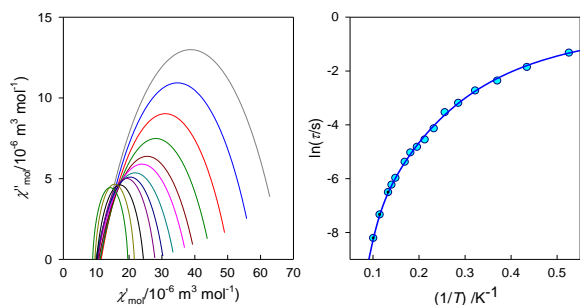


**Fig. 9.** The AC susceptibility data for **2** at  $B_{\text{DC}} = 0.2$  T. Left – Argand plot (fixed temperature between 1.9 and 9.9 K); right – Arrhenius-like plot with a fit to eqn. (2).

## Conclusion

Using a hexadentate Schiff-base ligand, a novel dinuclear  $[\text{Cu}^{\text{II}}\text{Dy}^{\text{III}}]$  complex has been synthesized and structurally characterized. The AC susceptibility measurements show that the complex exhibits slow magnetic relaxation typical for single-molecule magnets. Unusual is the fact that three relaxation processes exist in **1**; the slowest process at  $B_{\text{DC}} = 0.2$  T possesses the barrier to spin reversal  $U/k_{\text{B}} = 2.8$  K and the extrapolated relaxation time  $\tau_0 = 0.11$  s. The second process is typical for SMM of this class:  $U/k_{\text{B}} = 122$  K and  $\tau_0 = 1 \times 10^{-8}$  s; the third process (characterized upon an extrapolation) is even faster. The  $[\text{Co}^{\text{III}}\text{Dy}^{\text{III}}]$  complex, free of exchange coupling, exhibits only a single relaxation path with SMM parameters  $U/k_{\text{B}} = 113$  K,  $\tau_0 = 7.0 \times 10^{-9}$  s when direct, Raman, and Orbach processes are considered.

## Experimental Methods

### Chemicals and Reagents

Chemicals such as 3-methoxy-salicylaldehyde (*o*-vanillin), 2-hydroxy-1,3-diaminopropane,  $\text{Dy}(\text{NO}_3)_3$ ,  $\text{Dy}(\text{OAc})_3$  (Aldrich),  $\text{Cu}(\text{NO}_3)_2$ ,  $\text{Co}(\text{OAc})_2$  and triethylamine (TEA) (Merck, India) are of reagent grade and used without further purification. Solvents like methanol, ethanol (Merck, India) were of reagent grade and used as received.

### Synthesis of ligand $\text{H}_3\text{L}$

The Schiff base ligand was obtained by condensation of 2-hydroxy-1,3-diaminopropane (0.9 g, 10 mmol) and *o*-vanillin (3.04 g, 20 mmol) in ethanol with stirring at  $60^\circ\text{C}$  for 4 h, reported in our previous work<sup>17</sup>.

### Physical measurements

Elemental analyses were carried out using an automated elemental analyzer (Perkin-Elmer 240). IR spectra ( $400 - 4000$   $\text{cm}^{-1}$ ) were recorded in KBr pellets using FTIR spectrometer (Magna IR 750 series-II, Nicolet).



**Table 2.** Crystallographic data, details of data collection and structure refinement parameters for **1** and **2**

Molecular formula	C <sub>19</sub> H <sub>22</sub> CuDyN <sub>5</sub> O <sub>15</sub>	C <sub>25</sub> H <sub>35</sub> CoDyN <sub>2</sub> O <sub>14</sub> ·C <sub>2</sub> H <sub>3</sub> O <sub>2</sub> ·3(H <sub>2</sub> O)
Formula Weight	786.46	922.07
Crystal System	Monoclinic	Monoclinic
Space group	P21/c (No. 14)	P21/c (No. 14)
<i>a</i> /Å	9.0716(4)	11.1816(2)
<i>b</i> /Å	28.5414(12)	20.7429(4)
<i>c</i> /Å	10.2781(5)	15.4433(3)
$\alpha$ /deg	90	90
$\beta$ /deg	105.521(5)	102.707(1)
$\gamma$ /deg	90	90
<i>V</i> /Å <sup>3</sup>	2564.1(2)	3494.17(12)
<i>Z</i>	4	4
<i>D</i> (calc) /g cm <sup>-3</sup>	2.032	1.741
$\mu$ (MoK $\alpha$ ) /mm <sup>-1</sup>	3.806	2.679
<i>F</i> (000)	1536	1836
<i>T</i> /K	293	155
$\theta$ min, max /deg	3.2, 29.3	1.7, 27.6
Dataset	-12: 12 ; -39: 39 ; -14: 14	-14: 14 ; -27: 27 ; -20: 20
Tot., Uniq. Data, <i>R</i> (int)	26663, 7046, 0.052	58025, 8085, 0.035
Observed data [ <i>I</i> > 2 $\sigma$ ( <i>I</i> )]	5810	7112
<i>N</i> <sub>ref</sub> , <i>N</i> <sub>par</sub>	7046, 373	8085, 490
<i>R</i> , <i>wR</i> <sub>2</sub> , <i>S</i>	0.0530, 0.1175, 1.18	0.0277, 0.0788, 1.03
CCDC No	986119	1032248

### Single crystal X-ray diffraction

Single crystal X-ray data of complex **1** and **2** were collected on CCD diffractometer (SMART APEX-II, Bruker) using graphite monochromated MoK $\alpha$  radiation ( $\lambda = 0.71073$  Å). Data collection, reduction, structure solution, and refinement were performed using the Bruker Apex-II suite program. All available reflections to  $2\theta_{\max}$  were harvested and corrected for Lorentz and polarization factors with SAINT plus.<sup>18</sup> Reflections were then corrected for absorption, interframe scaling, and other systematic errors with SADABS.<sup>18</sup> The structures were solved by the direct methods and refined by means of full matrix least-square technique based on  $F^2$  with SHELX-97.<sup>19</sup> All the non-hydrogen atoms were refined with anisotropic thermal parameters. All hydrogen atoms on carbons were placed on their geometrically idealized positions, while hydrogen atom on the free -OH group was found on the difference Furrier map, and all of them were constrained to ride on

their parent atoms. The crystallographic data for **1** and **2** are given in **Table 1**.

### Magnetic Data Collection

The magnetic data was collected with the SQUID apparatus (MPMS-XL7, Quantum Design) using the RSO mode of detection with *ca* 30 mg of the sample encapsulated in a gelatine-made sample holder. The DC susceptibility taken at  $B = 0.1$  T has been corrected for the underlying diamagnetism. The magnetization has been measured at five temperatures  $T = 2.0 - 6.0$  K. The magnetization data was taken in the field-decreasing mode in order to eventually catch the remnant magnetization. The AC susceptibility measurements at different frequencies between  $\nu = 0.2 - 1512$  Hz were conducted at a working field  $B_{AC} = 0.38$  mT and an applied field  $B_{DC} = 0.2$  T, respectively. Twenty scans were averaged for each measurement. Data points outside the  $|0.5\sigma|$  interval were omitted, the rest was averaged and new standard deviation was calculated for the reduced data set.

### Synthesis of [Cu<sup>II</sup>Dy<sup>III</sup>(HL)(H<sub>2</sub>O)(NO<sub>3</sub>)<sub>3</sub>] (**1**)

A 20 cm<sup>3</sup> methanol solution of Cu(NO<sub>3</sub>)<sub>2</sub>·6H<sub>2</sub>O (0.263 g, 1.0 mmol) was added to a stirred solution of H<sub>3</sub>L(0.358 g, 1.0 mmol) and triethylamine base (TEA) (0.201 g, 2.0 mmol) in methanol (30 cm<sup>3</sup>) at room temperature. The resulting mixture was stirred for 10 min, and then finely powdered dysprosium nitrate (Dy(NO<sub>3</sub>)<sub>3</sub>) (0.438 g, 1.0 mmol) is added (Scheme 1). After being stirred for 1 h, the mixture was filtered to remove the precipitate, if any, and the clear green filtrate is then kept for slow evaporation. After a few days, green single crystals, suitable for crystal X-ray diffraction were deposited, which were then collected by filtration and washed with cold methanol. Color: light green. Yield: 0.510 g (65%). *Anal. calcd.* (%) for C<sub>19</sub>H<sub>22</sub>CuN<sub>5</sub>O<sub>15</sub>Dy: C 29.02, H 2.82, N 8.91; Found: C 29.38, H 2.78 and N 8.95. IR: 1627 vs cm<sup>-1</sup> for  $\nu$ (C=N), 3467 cm<sup>-1</sup> for  $\nu$ (alcoholic -OH);  $\nu$ (nitrate) 1470s, 1290s.

### Synthesis of [Co<sup>III</sup>Dy<sup>III</sup>(HL)(AcO)<sub>3</sub>(H<sub>2</sub>O)<sub>3</sub>](AcO)(H<sub>2</sub>O)<sub>3</sub> (**2**)

The complex **2** was synthesized following similar procedure as described for **1**, except use of Co(OAc)<sub>2</sub> and Dy(OAc)<sub>3</sub> instead of Cu(NO<sub>3</sub>)<sub>2</sub> and Dy(NO<sub>3</sub>)<sub>3</sub>, respectively. Color: dark brown. Yield: 0.714g (78%). *Anal. calcd.* (%) for C<sub>27</sub>H<sub>44</sub>CoN<sub>2</sub>O<sub>19</sub>Dy: C 35.17, H 4.81, N 3.04. Found: C 35.10, H 4.95 and N 3.25. IR: 1626vs cm<sup>-1</sup> for  $\nu$ (C=N), 3353bs cm<sup>-1</sup>

v(waters) and 3283vs v(alcoholic –OH); v(acetate) 1392s, 1328s.

## Acknowledgements

M. D. gratefully acknowledges UGC for the Fellowship (NET-SRF, direct). Financial support from CSIR (Ref. 02(2490)/11/EMR-II) and UGC [39-735/2010(SR)] New Delhi, are gratefully acknowledged. Grant Agencies (Slovakia: VEGA-1/0522/14, VEGA-1/0233/12, APVV-0014-11) are also acknowledged for the financial support.

## Notes and references

Electronic Supplementary Information (ESI) available: Crystallographic data in CIF format (CCDC no. 986119 and 1032248), tables of bond distances and angles, magnetic data and its analysis.

## References

- (a) W. Wernsdorfer and R. Sessoli, *Science*, 1999, **284**, 133; (b) R. Sessoli, H. L.Tsai, A. R. Schake, S. Y. Wang, J. B. Vincent, K. Folting, D. Gatteschi, G. Christou, and D. N. Hendrickson, *J. Am. Chem. Soc.* 1993, **115**, 1804; (c) A. Caneschi, D. Gatteschi, R. Sessoli, A. L. Barra, L. C. Brunel, and M. Guillot, *J. Am. Chem. Soc.* 1991, **113**, 5873–5874; (d) R. Sessoli, and A. K. Powell, *Coord. Chem. Rev.* 2009, **253**, 2328.
- (a) M. N. Leuenberger, and D. Loss, *Nature*, 2001, **410**, 789–793; (b) R. Sessoli, D. Gatteschi, A. Caneschi, and M. A. Novak, *Nature*, 1993, **356**, 141.
- (a) Y.-L. Miao, J.-L. Liu, J.-D. Leng, Z.-J. Lin, and M.-L. Tong, *CrystEngComm*, 2011, **13**, 3345; (b) X. J. Gu, R. Clérac, A. Hourri and D. F. Xue, *Inorg. Chim. Acta*, 2008, **361**, 3873.
- (a) A. Mishra, W. Wernsdorfer, K. A. Abboud, and G. Christou, *J. Am. Chem. Soc.* 2004, **126**, 15648; (b) C. M. Zaleski, E. C. Depperman, J. W. Kampf, M. L. Kirk, and V. L. Pecoraro, *Angew. Chem., Int. Ed.* 2004, **43**, 3912; (c) A. Okazawa, T. Nogami, H. Nojiri, T. Ishida, *Inorg. Chem.* 2008, **47**, 9763; (d) G. Novitchi, W. Wernsdorfer, L. F. Chibotaru, J. P. Costes, C. E. Anson, and A. K. Powell, *Angew. Chem., Int. Ed.* 2009, **48**, 1614; (e) J. Rinck, G. Novitchi, W. V. Heuvel, L. Ungur, Y. Lan, W. Wernsdorfer, C. E. Anson, L. F. Chibotaru, A. K. Powell, *Angew. Chem. Int. Ed.* 2010, **49**, 7583; (f) T. Kajiwara, M. Nakano, K. Takahashi, S. Takaishi, and M. Yamashita, *Chem. Eur. J.* 2011, **17**, 196.
- L. Sorace, C. Benelli, and D. Gatteschi, *Chem. Soc. Rev.* 2011, **40**, 3092 and refs cited therein.
- (a) G. Novitchi, J. P. Costes, J. P. Tuchagues, L. Vendier, W. Wernsdorfer, *New J. Chem.* 2008, **32**, 197; (b) T. Kajiwara, K. Takahashi, T. Hiraizumi, S. Takaishi, and M. Yamashita, *CrystEngComm*, 2009, **11**, 2110; (c) T. Kajiwara, M. Nakano, S. Takaishi, and M. Yamashita, *Inorg. Chem.*, 2008, **47**, 8604; (d) V. Baskar, K. Gopal, M. Helliwell, F. Tuna, W. Wernsdorfer, and R. E. P. Winpenny, *Dalton Trans.*, 2010, **39**, 4747; (e) J.-P. Costes, F. Dahan, and W. Wernsdorfer, *Inorg. Chem.*, 2006, **45**, 5. (f) S. Osa, T. Kido, N. Matsumoto, N. Re, A. Pochaba, and J. Mrozinski, *J. Am. Chem. Soc.*, 2004, **126**, 420; (g) J.-P. Costes, L. Vendier, and W. Wernsdorfer, *Dalton Trans.*, 2010, **39**, 4886; (h) C. Aronica, G. Pilet, G. Chastanet, W. Wernsdorfer, J. F. Jacquot, and D. Luneau, *Angew. Chem., Int. Ed.*, 2006, **45**, 4659; (i) C. Aronica, G. Chastanet, G. Pilet, B. Le Guennic, V. Robert, W. Wernsdorfer, and D. Luneau, *Inorg. Chem.*, 2007, **46**, 6108; (j) A. Okazawa, T. Nogami, H. Nojiri, and T. Ishida, *Chem. Mater.*, 2008, **20**, 3110; (k) A. Okazawa, T. Nogami, H. Nojiri, T. Ishida, *Inorg. Chem.*, 2009, **48**, 3292, (l) O. Iasco, G. Novitchi, E. Jeanneau, and D. Luneau, *Inorg. Chem.*, 2013, **52**, 8723.
- J. P. Costes, F. Dahan, A. Dupuis, and J. P. Laurent, *Inorg. Chem.*, 1997, **36**, 4284.
- (a) C. M. Zaleski, J. W. Kampf, T. Mallah, M. L. Kirk, and V. L. Pecoraro, *Inorg. Chem.*, 2007, **46**, 1954; (b) T. C. Stamatatos, S. J. Teat, W. Wernsdorfer, and G. Christou, *Angew. Chem., Int. Ed.*, 2009, **48**, 521; (c) V. Mereacre, A. M. Ako, R. Clérac, W. Wernsdorfer, I. J. Hewitt, C. E. Anson, A. K. Powell, *Chem. Eur. J.*, 2008, **14**, 3577; (d) A. Mishra, W. Wernsdorfer, S. Parsons, G. Christou, and E.K. Brechin, *Chem. Commun.*, 2005, 2086; (e) A. Mishra, A. J. Tasiopoulos, W. Wernsdorfer, E. E. Moushi, B. Moulton, M. J. Zaworotko, K. A. Abboud, and G. Christou, *Inorg. Chem.*, 2008, **47**, 4832.
- (a) M. N. Akhtar, V. Mereacre, G. Novitchi, J.-P. Tuchagues, C. E. Anson, and A. K. Powell, *Chem. Eur. J.*, 2009, **15**, 7278; (b) G. Abbas, Y. Lan, V. Mereacre, W. Wernsdorfer, R. Clérac, G. Buth, M. T. Sougrati, F. Grandjean, G. J. Long, C. E. Anson, and A. K. Powell, *Inorg. Chem.*, 2009, **48**, 9345; (c) M. Ferbinteanu, T. Kajiwara, K. Y. Choi, H. Nojiri, A. Nakamoto, N. Kojima, F. Cimpoesu, Y. Fujimura, S. Takaishi, and M. Yamashita, *J. Am. Chem. Soc.*, 2006, **128**, 9008.
- (a) E. M. Pineda, F. Tuna, R. G. Pritchard, A. C. Regan, R. E. P. Winpenny, and E. J. L. McInnes, *Chem. Commun.*, 2013, **49**, 3522; (b) Y.-Z. Zheng, M. Evangelisti, F. Tuna, and R. E. P. Winpenny, *J. Am. Chem. Soc.*, 2012, **134**, 1057; (c) Y.-Z. Zheng, M. Evangelisti, and R. E. P. Winpenny, *Chem. Sci.*, 2011, **2**, 99; (d) J.-P. Costes, L. Vendier, and W. Wernsdorfer, *Dalton Trans.*, 2011, **40**, 1700; (e) T. Yamaguchi, J.-P. Costes, Y. Kishima, M. Kojima, Y. Sunatsuki, N. Brefuel, J.-P. Tuchagues, L. Vendier, and W. Wernsdorfer, *Inorg. Chem.*, 2010, **49**, 9125; (f) L.-F. Zou, L. Zhao, Y.-N. Guo, G.-M. Yu, Y. Guo, J. Tang, and

- Y.-H. Li, *Chem. Commun.*, 2011, **47**, 8659; (g) X. Q. Zhao, Y. H. Lan, B. Zhao, P. Cheng, C. E. Anson, and A. K. Powell, *Dalton Trans.*, 2010, **39**, 4911; (h) V. Gómez, L. Vendier, M. Corbella, and J.-P. Costes, *Inorg. Chem.*, 2012, **51**, 6396; (i) K. C. Mondal, A. Sundt, Y. Lan, G. E. Kostakis, O. Waldmann, L. Ungur, L. F. Chibotaru, C. E. Anson, and A. K. Powell, *Angew. Chem., Int. Ed.*, 2012, **51**, 7550; (j) G. J. Sopsis, M. Orfanoudaki, P. Zampas, A. Philippidis, M. Siczek, T. Lis, J. R. O'Brien, and C. J. Milios, *Inorg. Chem.*, 2012, **51**, 1170; (k) M. Towatari, K. Nishi, T. Fujinami, N. Matsumoto, Y. Sunatsuki, M. Kojima, N. Mochida, T. Ishida, N. Re, and J. Mrozinski, *Inorg. Chem.*, 2013, **52**, 6160; (l) J. P. Costes, F. Dahan, J. García-Tojal, *Chem. Eur. J.*, 2002, **8**, 5430; (n) F. Mori, T. Nyui, T. Ishida, T. Nogami, K.-Y. Choi, and H. Nojiri, *J. Am. Chem. Soc.*, 2006, **128**, 1440; (o) H. L. C. Feltham, R. Clerac, L. Ungur, V. Vieru, L. F. Chibotaru, A. K. Powell, and S. Brooker, *Inorg. Chem.*, 2012, **51**, 10603; (p) J. Fraser, F. J. Kettles, V. A. Milway, F. Tuna, R. Valiente, L. H. Thomas, W. Wernsdorfer, S. T. Ochsenbein, and M. Murrie, *Inorg. Chem.*, 2014, **53**, 8970.
- 11 (a) N. Ishikawa, M. Sugita, T. Ishikawa, S. Koshihara, and Y. Kaizu, *J. Phys. Chem. B*, 2004, **108**, 11265; (b) A. Abragam, and B. Bleaney, *Electron Paramagnetic Resonance of Transition Ions*; Clarendon Press: Oxford, 1970; (c) K. J. Standley, and R. A. Vaughan, *Electron Spin Relaxation Phenomena in Solids*; Hilger: London, 1969.
- 12 (a) A. V. Funes, L. Carrella, E. Rentschler, and P. Alborés, *Dalton Trans.*, 2014, **43**, 2361; (b) J. D. Rinehart, K. R. Meihaus, and J. R. Long, *J. Am. Chem. Soc.*, 2010, **132**, 7572; (c) C.-M. Liu, D.-Q. Zhang, and D.-B. Zhu, *Inorg. Chem.*, 2013, **52**, 8933; (d) V. Chandrasekhar, S. Hossain, S. Das, S. Biswas, and J.-P. Sutter, *Inorg. Chem.*, 2013, **52**, 6346; (e) R. Boča, J. Miklovič, and J. Titiš, *Inorg. Chem.*, 2014, **53**, 2367.
- 13 R. Boča, *A Handbook of Magnetochemical Formulae*; Elsevier: Amsterdam, 2012.
- 14 J. M. Zadrozny, M. Atanasov, A. M. Bryan, C.-Y. Lin, B. D. Reinken, P. P. Power, F. Neese, and J. R. Long, *Chem. Sci.* **2013**, **4**, 125.
- 15 (a) G. Poneti, K. Bernot, L. Bogani, A. Caneschi, R. Sessoli, W. Wernsdorfer, and D. Gatteschi, *Chem. Commun.*, 2007, 1807; (b) V. Chandrasekhar, B. M. Pandian, J. J. Vittal, and R. Clérac, *Inorg. Chem.*, 2009, **48**, 1148; (c) T. D. Pasatou, M. Etienne, A. M. Madalan, M. Andruh, and R. Sessoli, *Dalton Trans.*, 2010, **39**, 4802; (d) K. Xiang, Y. Lan, H.-Y. Li, L. Jiang, T.-B. Lu, C. E. Anson, and A. K. Powell, *Dalton Trans.*, 2010, **39**, 4737; (e) Z. Majeed, K. C. Mondal, G. E. Kostakis, Y. Lan, C. E. Anson, and A. K. Powell, *Dalton Trans.*, 2010, **39**, 4740; (f) P.-H. Lin, I. Korobkov, W. Wernsdorfer, L. Ungur, L. F. Chibotaru, and M. Murugesu, *Eur. J. Inorg. Chem.*, 2011, 1535; (g) J. Long, F. Habib, P.-H. Lin, I. Korobkov, G. Enright, L. Ungur, W. Wernsdorfer, L. F. Chibotaru, and M. Murugesu, *J. Am. Chem. Soc.*, 2011, **133**, 5319; (h) S. K. Langley, N. F. Chilton, L. Ungur, B. Moubaraki, L. F. Chibotaru, and K. S. Murray, *Inorg. Chem.*, 2012, **51**, 11873; (i) G. Abbas, G. E. Kostakis, Y. Lan, and A. K. Powell, *Polyhedron*, 2012, **41**, 1; (j) M. U. Anwar, L. K. Thompson, L. N. Dawe, F. Habib, and M. Murugesu, *Chem. Commun.*, 2012, **48**, 4576; (k) N. M. Randell, M. U. Anwar, M. W. Drover, L. N. Dawe, and L. K. Thompson, *Inorg. Chem.*, 2013, **52**, 6731; (l) S.-Y. Jhan, S.-H. Huang, C.F.-I. Yang, and H.-L. Tsai, *Polyhedron*, 2013, **66**, 222; (m) S. K. Langley, N. F. Chilton, B. Moubaraki, and K. S. Murray, *Polyhedron*, 2013, **66**, 48; (n) S. K. Langley, B. Moubaraki, and K. S. Murray, *Polyhedron*, 2013, **64**, 255; (o) J. Kan, H. Wang, W. Sun, W. Cao, J. Tao, and J. Jiang, *Inorg. Chem.*, 2013, **52**, 8505; (p) J. Feuersenger, D. Prodius, V. Mereacre, R. Clérac, C. E. Anson, and A. K. Powell, *Polyhedron*, 2013, **66**, 257; (q) J. Robin, R. J. Blagg, L. Ungur, F. Tuna, J. Speak, P. Comar, D. Collison, W. Wernsdorfer, E. J. L. McInnes, L. F. Chibotaru, and R. E. P. Winpenny, *Nature Chemistry*, 2013, **5**, 673; (r) D. N. Woodruff, R. E. P. Winpenny, R. A. Layfield, *Chem. Rev.*, 2013, **113**, 5110; (s) Sk. Md. T. Abtab, M. C. Majeed, M. Maity, J. Titiš, R. Boča, and M. Chaudhury, *Inorg. Chem.*, 2014, **53**, 1295.
- 16 F. Neese et al., Program ORCA 3.0.3. B88-LYP calculations, 62 atoms, 386 electrons, ZORA-TZV basis set (GTO), 555 contracted basis functions, grid4 algorithm, UHF mult = 7, exchange convention  $\hat{H}^{\text{ex}} = -2J(\vec{S}_1 \cdot \vec{S}_2)$ .
- 17 M. Dolai, T. Mistri, A. Panja, and M. Ali, *Inorg. Chimica Acta*, 2013, **399**, 95.
- 18 (a) SMART (V 5.628), SAINT (V 6.45a), XPREP, SHELXTL, Bruker AXS Inc., Madison, WI, 2004; (b) G. M. Sheldrick, *SADABS (Version 2.03)*, University of Gottingen, Germany, 2002.
- 19 (a) G. M. Sheldrick, *SHELXS-97*, *Acta Crystallogr.* 2008, **A64**, 112; (b) A. L. Spek, *Acta Crystallogr.* 2009, **D65**, 148.



## TOC FILE

**Cu(II)-Dy(III) and Co(III)-Dy(III) based single molecule magnets with multiple slow magnetic relaxation processes in Cu(II)-Dy(III) complex**

Malay Dolai, Mohammad Ali, Ján Titiš and Roman Boča

Two Cu<sup>II</sup>-Dy<sup>III</sup> and Co<sup>III</sup>-Dy<sup>III</sup> dinuclear complexes of a Schiff base ligand (H<sub>3</sub>L) exhibit single-molecule magnetic behaviour with multiple slow magnetic relaxation processes for the former.

